J. theor. Biol. (1993) **162**, 23–40

Chemical Control of Eukaryotic Cell Movement: A New Model

JONATHAN A. SHERRATT†, E. HELENE SAGE‡ AND J. D. MURRAY§

† *Centre for Mathematical Biology, Mathematical Institute, 24–29 St Giles', Oxford OX1 3LB, U.K.,* ‡ *Department of Biological Structure SM-20 and* § *Department of Applied Mathematics FS-20, University of Washington, Seattle, WA 98195, U.S.A.*

(*Received on 1 February* 1992, *Accepted in revised form on 7 October* 1992)

Cellular chemotaxis and chemokinesis play important roles in many biological processes. Most continuum mathematical models for these regulatory mechanisms are based on the model of Keller & Segel (1971*a*, *b*), in which cells respond directly to the local concentration of extracellular chemical. We have developed a new model which reflects the receptor-based mechanisms underlying chemical control of cell motion. Our model consists of three coupled partial differential equations, and we use the Boyden chamber (millipore) assay to compare it with a simpler model based on the Keller–Segel approach. The predictions of our model capture the key qualitative features of the experimental data, whereas the simpler model only does so when appropriate functional forms are chosen for the dependence of the transport coefficients on chemical concentration. Using experimental data on the variation of receptor kinetic parameters with temperature, we use our model to predict the effect of decreasing the temperature on both the "leading front" and "migrated cell" measurements taken from Boyden chamber assays. Our results show that changes in the kinetic parameters play a key role in controlling the temperature dependence of cell chemotaxis and chemokinesis.

Biological Background and Previous Models

Chemical regulation of cell movement is important in a wide range of biological processes, and its roles in the immune response, developmental control, and the aggregation of cellular slime moulds are particularly well documented. The current terminology in the subject was established by Keller *et al.* (1977). They defined chemokinesis as "a reaction by which the speed or frequency of locomotion and/or the frequency and magnitude of turning of cells or organisms moving at random is determined by substances in the environment", whereas chemotaxis was "a reaction by which the direction of locomotion of cells or organisms is determined by substances in their environment". Although there is still debate in the literature on some finer points of the interpretation of these definitions (Bignold, 1988*a*; Wilkinson, 1988*a*, *b*), the terms are now in widespread use.

The available experimental evidence, which is reviewed in detail by Devreotes & Zigmond (1988), suggests that chemotaxis and chemokinesis occur in eukaryotic cells via the binding of regulatory chemicals to receptors on the cell surface; the number and location of bound receptors modulates pseudopod extension and thus cell motion (Zigmond, 1989). The systems that have been studied in most detail are the response

0022–5193/93/090023+18 $08.00/0

of polymorphonuclear leukocytes to N-formylated peptides and of *Dictyostelium discoideum* amoebae to cyclic AMP. The mechanisms in the two cases are remarkably similar. The receptor–chemical complex is rapidly internalized in intracellular vesicles, and once inside the cell it dissociates, to yield free intracellular chemical and receptor. Experiments and modelling by Zigmond *et al.* (1982) suggest that in at least the leukocyte–peptide system, the intracellular chemical is partitioned into two pools, with a proportion of the chemical degraded and released, and the remainder kept in a long-term "storage pool". In some instances, the internalized receptors appear to be recycled back to the cell surface (Sullivan & Zigmond, 1980; Van Haarstert, 1987); moreover, in the presence of extracellular regulatory chemical, additional receptors (up to 30-fold) can be released to the cell surface from an intracellular pool (Fletcher & Gallin 1980; Janssens & Van Driel, 1984; Zimmerli *et al.*, 1986).

A number of mathematical models have been proposed for chemically modulated cell movement. The oldest and most widely used is the continuum model of Keller & Segel (1971*a*, *b*). They take the cell flux J_n to be directly dependent on the local extracellular chemical concentration, *via* the expression

$$J_n = \underbrace{-D_n(c)\nabla n}_{\text{Chemokinesis}} + \underbrace{\chi_n(c)n\nabla c}_{\text{Chemotaxis and chemokinesis}}, \qquad (1)$$

where n and c are the local cell density and chemical concentration, respectively, and the transport coefficients $D_n(c)$ and $\chi_n(c)$ are strictly positive for all c. Since variations in c affect both the magnitude and direction of the second term, this term represents a combination of chemotaxis and chemokinesis effects, under the definitions of Keller *et al.* (1977). This model was originally applied by Keller & Segel (1971*a*, *b*) to bacterial movement, but has more recently been used with considerable success in a wide range of cellular and whole organism applications. The Keller–Segel approach takes no account of the role of receptor kinetics in the cellular response to chemotactic and chemokinetic factors: indeed, these kinetics were very poorly understood when the model was formulated. More recently, Segel (1976) incorporated receptor kinetics into the model when applied to bacterial movement. His model consists of nine coupled partial differential equations, and a simplification reducing the system to six equations is considered in a second paper (Segel, 1977). Subsequent experimental work on receptor modification in bacteria is reflected in the models of Goldbeter & Koshland (1982) and Segel *et al.* (1986). However, this work has little relevance to eukaryotic cells, since the receptor-based mechanisms responsible for chemotaxis are quite different in the two cell types. In particular, eukaryotic cells respond to spatial gradients in the chemoattractant, while bacteria can only modify the length of time they spend moving in a particular direction, in response to a temporal gradient of chemical concentration.

At the single cell level, Tranquillo and coworkers have developed a detailed stochastic model for the motion of a single leukocyte in the presence of chemoattractants (Tranquillo & Lauffenburger, 1987; Tranquillo *et al.*, 1988; Tranquillo, 1990). This model applies exclusively to a single cell, but in an attempt to combine single cell

and cell population models, Rivero *et al.* (1989) proposed a continuum model in which the transport coefficients are related to the parameters of a simple stochastic model for the movement of an individual cell. Yet another approach is used by Lauffenburger and coworkers (Fisher & Lauffenburger, 1987; Charnick & Lauffenburger, 1990; Charnick *et al.*, 1991) who take cell-cell encounters to be determined by a random walk that is biased owing to chemotaxis.

Modelling the Boyden Chamber Assay

The Boyden chamber assay is a relatively simple *in vitro* system which enables chemotactic and chemokinetic effects to be tested quantitatively. The assay was developed by Boyden (1962), and its subsequent use is reviewed by Bignold (1988*b*). It consists of two wells separated by a thin filter whose porosity enables cells to crawl actively through, but prevents passive falling of cells under gravity between the upper and lower wells (Fig. 1). The lower well is filled with a solution of the chemical under test, and the filter is placed on top of this well; the pores of the filter rapidly fill with the chemical solution, owing to capillary action. The upper well is then filled with a suspension of the cells under test, and the cells rapidly settle onto the top of the filter. The system is left for a given length of time (about an hour), during which the cells crawl through the filter in response to the concentration gradient in the regulatory chemical. Having passed through the filter, the cells rapidly spread across the lower surface of the filter, and at the end of the given time period, the number of cells on the lower surface of the filter is counted. An alternative approach, first suggested by Zigmond & Hirsch (1973), is to use a thicker filter, and measure the distance travelled by the leading cell front in the given time period. To distinguish between chemotaxis and chemokinesis, the experiment is often repeated with the cells in the upper well suspended in a solution of the chemical under test. A chemical gradient will then only arise owing to cellular degradation of active chemical.

We begin by applying a model based on that of Keller & Segel (1971*a*, *b*) to chemically controlled cell movement in the Boyden chamber assay. Previously,

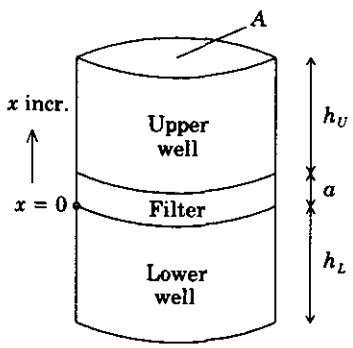

FIG. 1. A diagrammatic representation of the Boyden chamber assay. The upper and lower wells have height h_U and h_L, respectively, and the filter has thickness a. Both wells and filter have cross-sectional area A. We take x to be distance measured vertically, with $x = 0$ the lower surface of the filter.

Lauffenburger & Zigmond (1981) and Lauffenburger *et al.* (1988) have solved the diffusion equation to predict the chemical concentration as a function of time in the filter and wells of the Boyden chamber, and Buettner *et al.* (1989*a*, *b*) have applied the Keller–Segel approach to leukocyte movement in the Boyden chamber assay. We will compare the model predictions with the typical experimental data of Harvath & Aksamit (1984) to estimate the transport coefficients in the model. Harvath & Aksamit (1984) studied the motile response of human neutrophils to concentration gradients of the peptide N-formyl-methionyl-leucyl-phenylalanine (FMLP), which has important implications for the inflammatory response to injury; their results are illustrated in Fig. 2. The qualitative feature of bell-shaped dose–response curves has been found in Boyden chamber studies for a range of chemicals and cell types, in a variety of Boyden chambers (see Bignold, 1988*b* for references).

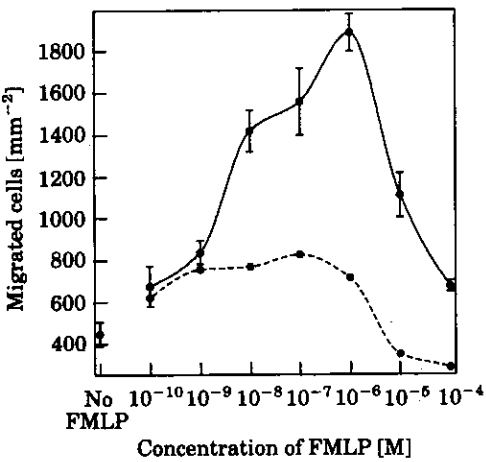

FIG. 2. The experimental results of Harvath & Aksamit (1984) on the movement of human neutrophils through a Boyden chamber in response to gradients of FMLP. The number of cells on the lower surface of the filter after 60 min is plotted against the initial concentration of FMLP in the lower well, c_L. For clarity, these concentrations are plotted on a logarithmic scale. The dimensions of the chamber were, in the notation of Fig. 1, $h_L = 3{\cdot}125$ mm, $h_U = 6{\cdot}25$ mm, $a = 10$ μm and $A = 7$ mm^2, and 25 000 cells were initially added to the upper well, suspended in Hank's balanced salt solution; the peptide was also in solution with Hank's balanced salt solution. The filters were polycarbonate, free of polyvinylpyrrolidone, with 5 μm pores. The chambers were incubated for 60 min at 37°C in humidified air with 5% CO_2. The filters were then removed and stained with Diff-Quik, and the cells on the lower surface of the filter were counted. The data points (•) denote the mean experimental result, and the error bars represent the standard deviation of the means. (——FMLP added to upper well only; - - - FMLP added to both wells).

Following Keller & Segel (1971*a*, *b*), we use the representation (1) for chemically controlled cell flux, and our model consists of two partial differential equations:

$$\frac{\partial n}{\partial t} = \frac{\partial}{\partial x}\left[D_n(c)\frac{\partial n}{\partial x}\right] - \frac{\partial}{\partial x}\left[\chi_n(c) n \frac{\partial c}{\partial x}\right] \tag{2a}$$

$$\frac{\partial c}{\partial t} = D_c \frac{\partial^2 c}{\partial x^2} \tag{2b}$$

where $n(x, t)$ and $c(x, t)$ are the local cell density and chemical concentration, respectively, x is distance measured vertically, and t is time. The first of these is a conservation equation for cells, while the second is simply the diffusion equation. The dependence of the transport coefficients D_n and χ_n on c will be estimated using the data of Harvath & Aksamit (1984). We take $x=0$ as the lower surface of the filter, and neglect any horizontal variations, which is a reasonable approximation, since the cross-sectional diameter of the chamber is very much larger than the thickness of the filter. The chemical diffuses throughout the upper and lower wells and the filter, so that c is defined on $-h_L<x<h_U+a$ (notation as in Fig. 1), with zero flux boundary conditions at the endpoints. We assume that the diffusion of FMLP is unaffected by the presence of the filter, since its molecules are many orders of magnitude smaller than the pores of the filter, which have a diameter of 5 μm.

Cell movement is restricted to the filter region of the chamber, so that n is defined only on $0\leq x\leq a$. Thus we solve eqn (2a) on $[0, a]$ and eqn (2b) on $[-h_L, h_U+a]$. The cells on the upper and lower surfaces of the filter occupy a layer of thickness one cell diameter, L say, which for human neutrophils is about 9 μm (Lentz, 1971; Tatsuo & Kobayashi, 1972). The accumulation of cells on the lower surface occurs at rate $-J_nA$, where J_n is given by (1); J_n is negative since the cell flux is in the direction of decreasing x. Cell conservation and the continuity of n therefore imply that the appropriate boundary condition at $x=0$ is $\partial n/\partial t=-J_n/L$, and similarly $\partial n/\partial t=J_n/L$ at $x=a$. The appropriate initial conditions are $c=c_L$ on $-h_L<x<a$, $c=c_U$ on $a\leq x<h_U+a$, and $n=0$ on $0\leq x<a$ with $n=n_0\equiv N_0/(L\,.\,A)$ at $x=a$; here c_U and c_L are the initial concentrations of chemical in the upper and lower wells, respectively, and N_0 is the number of cells initially added to the upper well. Given the short duration of the experiment, we neglect any effects of cell division. We also neglect any degradation of chemical by the cells; Lauffenburger *et al.* (1988) have suggested including a degradation term dependent on n and c in (2b) when applied to the Boyden chamber assay, but we postpone inclusion of such a term until the development of our new model, which is based on the receptor mechanisms responsible for this degradation.

The value of the chemical diffusion coefficient D_c can be estimated theoretically. A straightforward calculation using kinetic theory and Stokes' law for viscous drag implies that the diffusion coefficient of a solute in aqueous solution is given by

$$D_{\text{theor}}=\frac{kT}{6\pi\eta}\cdot\left[\frac{4\pi N_A}{3Mv}\right]^{1/3} \tag{3}$$

(Barrow, 1981; Berg & Von Hippel, 1985). Here k is the Boltzmann constant, T is the absolute temperature, η is the viscosity of water at temperature T, v is the specific volume of the solute, M is the molecular weight of the solute, and N_A is the Avogadro constant. This formula gives the value $D_c=7{\cdot}3\times10^{-6}\ \text{cm}^2\ \text{sec}^{-1}$ for FMLP at 37°C; a similar estimate was made by Lauffenburger & Zigmond (1981).

With this estimate for D_c, we can use the data of Harvath & Aksamit (1984) to predict the dependence of the transport coefficients D_n and χ_n on the concentration c of FMLP. To do this, we set $X_n=0$ and fit the model predictions of the value of

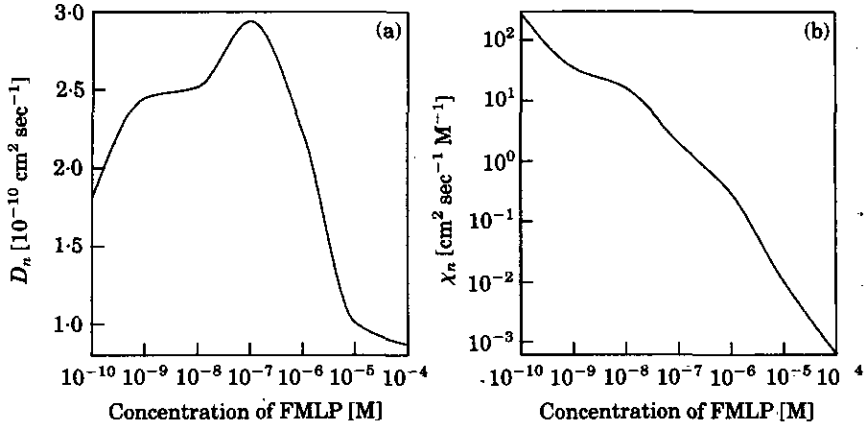

FIG. 3. The variation of the transport coefficients (a) $D_n(c)$ and (b) $\chi_n(c)$ of human neutrophils with the concentration c of FMLP, as predicted by the model (2) and the data of Harvath & Aksamit (1984), which is illustrated in Fig. 2. The remaining parameter D_c is calculated theoretically using (3). Equation (2) was solved analytically using Fourier transforms, under the approximation $h_U = h_L = \infty$ (recall that $h_U, h_L \gg a$). Equation (2a) was then solved numerically using a semi-implicit finite difference scheme, and the solutions for different values of c_U and c_L were used to estimate $D_n(c)$ and $\chi_n(c)$, as discussed in the text. In the case $c_U = 0$, we neglect variations in D_n and χ_n across the filter, since at times greater than 2 min after the experiment, c varies by less than 1% across the filter, while D_n and χ_n do not vary too rapidly with c. For clarity, we plot c and χ_n on logarithmic scales.

$n(x=0,\ t=1\text{ hr})$ to the data in the case $c_U = c_L$, so that $c(x,t) \equiv c_L$; this determines $D_n(c)$. The data for $c_U = 0$ can then be used to determine $\chi_n(c)$. These estimated variations in the transport coefficients are illustrated in Fig. 3, and a typical model solution is shown in Fig. 4. From this approach, it is clear that the Boyden chamber assay provides a straightforward way of obtaining quantitative estimates for the cellular transport coefficients in a model based on the Keller–Segel flux (1). However,

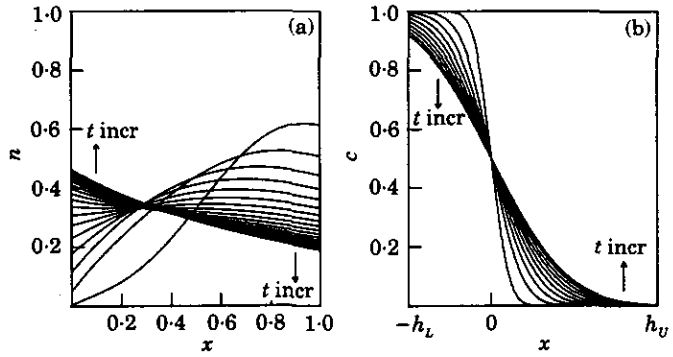

FIG. 4. The solution for $n(x,t)$ and $c(x,t)$ of (2) when $c_U = 0$ and $c_L = 10^{-8}$ M. We plot the solutions as functions of x at time intervals of 3 min for n and 6 min for c. The parameters $D_n(c)$ and $\chi_n(c)$ are as in Fig. 3, and the chemical diffusion coefficient D_c is estimated theoretically using (3). The solution was determined as in Fig. 3. (a) $n(x,t)$ in filter; (b) $c(x,t)$ in filter and wells.

the assay also highlights the necessity of externally specifying the parameter variations illustrated in Fig. 3 before a model based on (1) can be applied to a biological system. These parameter variations are in fact determined by the receptor kinetics controlling cell–chemical interactions, and in the remainder of this study we develop a new model which incorporates these receptor kinetics.

Receptor Kinetics and a New Model

The interaction between the receptors for a movement regulating chemical on the surface of a eukaryotic cell and the molecules of that chemical can be reasonably represented by the following simple scheme:

$$\begin{matrix}\text{Extracellular} \\ \text{chemical}\end{matrix} + \begin{matrix}\text{Receptors on} \\ \text{the cell surface}\end{matrix} \underset{k_d}{\overset{k_a}{\rightleftharpoons}} \begin{matrix}\text{Bound receptor–} \\ \text{chemical complex}\end{matrix} \overset{k_i}{\rightarrow} \begin{matrix}\text{Internalized receptor–} \\ \text{chemical complex}\end{matrix}$$

(Sullivan & Zigmond, 1980; Zigmond *et al.*, 1982; Omann *et al.*, 1987). Here k_a, k_d and k_i are, respectively, the rate constants for the processes of association, dissociation and internalization of the receptor–chemical complex on the cell surface. In the absence of spatial variations, the law of mass action then implies

$$\frac{\partial c}{\partial t} = k_d u - k_a c R \tag{4a}$$

$$\frac{\partial u}{\partial t} = k_a c R - k_d u - k_i u. \tag{4b}$$

Here $c(r, t)$, $R(r, t)$ and $u(r, t)$ are the concentrations of extracellular chemical, free receptors and bound receptors per unit volume at position r and time t; the dynamics of $R(r, t)$ are discussed below. Following Zigmond (1981), we assume that the chemotactic effect of the chemical is a result of differences in the number of bound receptors on opposite sides of a cell, while chemokinesis occurs as a response to the total number of bound receptors. We therefore take the local cell flux to be given by

$$J_n = -\underbrace{D(\rho)\nabla n}_{\substack{\text{Random migration} \\ \text{and chemokinesis}}} + \underbrace{\chi n \nabla \rho}_{\substack{\text{Chemotaxis} \\ \text{and chemokinesis}}} \tag{5}$$

where $n(r, t)$ is the local cell density and $\rho(r, t)$ is the number of moles of bound receptor per cell. The second term in (5) is dependent both on the magnitude and direction of $\nabla\rho$, and thus represents a combination of chemotaxis and chemokinesis under the definitions of Keller *et al.* (1977), which were discussed in the Introduction. Moderate concentrations of FMLP have a positive chemokinetic effect on human neutrophils. However, a large number of studies, including that of Harvath & Aksamit (1984), whose results are illustrated in Fig. 2, have found a reduction in random motility at high peptide concentrations. We therefore take $D(\rho)$ to be an inverted parabola, with the form $D(\rho) = D_0 + D_1\rho - D_2\rho^2$, where D_0, D_1 and D_2 are positive constants.

Movement of receptors in space occurs only via passive convection with the cells, so that the flux of bound receptors at any point is given by ρJ_n. Substituting these expressions for spatial flux into (4) gives

$$\frac{\partial n}{\partial t} = -\nabla . J_n \tag{6a}$$

$$\frac{\partial c}{\partial t} = D_c \nabla^2 c + k_d u - k_a c R \tag{6b}$$

$$\frac{\partial u}{\partial t} = -\nabla . (\rho J_n) + k_a c \dot{R} - k_d u - k_i u, \tag{6c}$$

whereas in the previous section, D_c is the diffusion coefficient of the extracellular chemical. The relationship between ρ and u is discussed below. The dynamics of R, the number of free receptors per unit volume, depends on the processes of intracellular recycling of receptors and release of receptors from an intracellular pool, as discussed in the Introduction. Though only partially understood, these processes are known to be extremely complex, and have been modelled in detail by a number of previous authors. In particular, Zigmond *et al.* (1982) investigated the kinetics of intracellular processing of peptide receptors on leukocytes. Despite a number of simplifications, their model consists of seven coupled non-linear differential equations. In common with other, less specific models of receptor processing (Gex-Fabry & Delisi, 1984; Linderman & Lauffenburger, 1989), these equations address only the intracellular kinetics, and make no reference to the effects on cell movement. There is also an extensive literature on the mathematical modelling of intercellular communication by cyclic AMP waves in *D. discoideum* (Martiel & Goldbeter, 1987; Monk & Othmer, 1989; Tyson & Murray, 1989). Again, these are complex models which take no account of cell movement. Moreover, the quantitative data available on the rates at which receptor recycling and release occur are extremely limited.

Therefore, rather than adding a large number of additional equations and unknown parameters to (6) in an attempt to take R as a dependent variable of the model, we assume that the total number of receptors (bound or free) on the cell surface is an increasing function of the number of bound receptors. That is, we assume that $R+u=n\Gamma f(\rho)$, where the constant Γ is the total number of moles of (free) receptors on a cell in the absence of any chemical, and $f(0)=1$. We require $f(\rho)$ to be an increasing function, and in the absence of detailed experimental data, we take it to be linear, so that $f(\rho)=1+\beta\rho$. The parameter β is determined by the constraint of a finite supply of receptors in the intracellular pool, so that there is a maximum number of receptors, $\rho_{\max}$ say, that can be expressed on the cell surface. This maximum level of expression will only be attained in the limit as all these receptors become occupied, so that $\rho_{\max}=\Gamma(1+\beta\rho_{\max})$.

With this expression for $R(r, t)$, (6) is a system of three coupled partial differential equations for four dependent variables, namely cell density $n(r, t)$, extracellular chemical concentration $c(r, t)$, bound receptor concentration per unit volume $u(r, t)$, and the number of moles of bound receptor per cell $\rho(r, t)$. However, we have the

additional relation that when $n \neq 0$, $\rho = u/n$; when $n = 0$, ρ is undefined. Therefore, when $n \neq 0$,

$$\frac{\partial \rho}{\partial t} = \frac{1}{n}\frac{\partial u}{\partial t} - \frac{u}{n^2}\frac{\partial n}{\partial t}$$

$$= -\frac{1}{n} J_n \cdot \nabla \rho + \Gamma k_a c(1 + \beta\rho) - k_a c\rho - (k_d + k_i)\rho \qquad (7)$$

using (6a) and (6c). Henceforth, we take n, c and ρ as the dependent variables. The model can also be expressed in terms of n, c and u, but the resulting conservation equation for u contains a backwards diffusion term, which results in unbounded numerical solutions.

We now consider applying this model to the Boyden chamber assay. As in the case of the simple model (2) discussed in the previous section, the variable c is defined in both the wells and the filter, that is $-h_L \leq x \leq h_U + a$ in the notation of Fig. 1, while n is defined only within the filter, $0 \leq x \leq a$. In the case of a simple linear diffusion equation, it is well known that sharp fronts cannot exist within the domain of solution. Similar arguments for our system show that the inequality $n(x, t) > 0$ holds on $0 \leq x \leq a$ for all $t > 0$, so that ρ is defined on $0 \leq x \leq a$ for all $t > 0$. Therefore eqn (6) applies on the whole of $0 \leq x \leq a$ for all $t > 0$. In the well regions, the concentration of chemical c satisfies the diffusion equation, $\partial c/\partial t = D_c \partial^2 c/\partial x^2$; we require continuity of chemical flux, $\partial c/\partial x$, at the ends $x = 0$ and $x = a$ of the filter, with $\partial c/\partial x = 0$ at $x = -h_L, h_U + a$. As in the previous section, we take the boundary conditions satisfied by the cell density to be $\partial n/\partial t = -J_n/L$ at $x = 0$ and $\partial n/\partial t = J_n/L$ at $x = a$. The number of bound receptors on the lower surface of the filter increases during the experiment, owing to convective accumulation and kinetic changes, and a straightforward calculation shows that $\partial \rho/\partial t = \Gamma k_a c(1 + \beta\rho) - k_a c\rho - (k_d + k_i)\rho$ at $x = 0$, a. Comparing this with (7) implies that $\partial \rho/\partial x = 0$ at the two endpoints.

Parameter Values and Non-dimensionalization

In our discussion of the simple model (2), we established the dimensional parameter values $D_c = 7{\cdot}3 \times 10^{-6}\,\mathrm{cm^2\,sec^{-1}}$ and $L = 9\,\mu\mathrm{m}$. We will determine the values of the transport coefficients D_0, D_1, D_2 and χ by comparing the model predictions with the data of Harvath & Aksamit (1984), but we must first obtain estimates for the parameters k_a, k_d, k_i, Γ and $\rho_{\max}$, which reflect the number and kinetics of the FMLP receptors on the neutrophil surface. The kinetics have been studied in detail by several authors, and are highly temperature dependent: for example, internalization is essentially blocked at 4°C. We base our parameters on the data of Sklar *et al.* (1984), who found appropriate values for the rate constants at 37°C to be $k_a = 10^9\,\mathrm{M^{-1}\,min^{-1}}$, $k_i = 0{\cdot}24\,\mathrm{min^{-1}}$ and $k_d = 0{\cdot}35\,\mathrm{min^{-1}}$; the binding kinetics are therefore quite fast compared to the time scale of cell movement in this case. Their study also revealed complexities in the kinetics, notably a variation in the rates of dissociation and internalization according to the duration of binding, but we neglect such complications. For Γ and $\rho_{\max}$, recall that Γ is the number of moles of (free) receptor

on the cell surface in the absence of chemical, while $\rho_{\max}$ is the upper limit on the total number of moles of receptor (free or bound) on the cell surface, owing to the finite nature of the intracellular pool of receptors. Measurements of the total number of FMLP receptors on neutrophils vary widely, from about 3000 to about 100000 (Williams *et al.*, 1977; Zimmerli *et al.*, 1986; Follin *et al.*, 1989). Therefore, we take $\Gamma = 3000/6{\cdot}02 \times 10^{23} = 4{\cdot}98 \times 10^{-21}$ mol and $\rho_{\max} = 33\frac{1}{3}\Gamma$, which gives $\beta = 0{\cdot}97/\Gamma$.

Having established these parameter values, we non-dimensionalize the model (6a, b) and (7) by defining the following dimensionless quantities, denoted by*.

$$n^* = n/n_0 \qquad c^* = c/c_L \qquad \rho^* = \rho/\Gamma \qquad x^* = x/a \qquad t^* = t/T \qquad D_0^* = D_0 T/a^2$$
$$D_1^* = D_1 T\Gamma/a^2 \qquad D_2^* = D_2 T\Gamma^2/a^2 \qquad D_c^* = D_c T/a^2 \qquad \chi^* = \chi T\Gamma/a^2$$
$$k_a^* = k_a T c_L \qquad k_d^* = k_d T \qquad k_i^* = k_i T \qquad \Gamma^* = \Gamma n_0/c_L \qquad \rho_{\max}^* = \rho_{\max}/\Gamma$$
$$\beta^* = \beta\Gamma \qquad h_L^* = h_L/a \qquad h_U^* = (h_U + a)/a \qquad c_U^* = c_U/c_L \qquad J_n^* = J_n T/(n_0 a);$$

we take the time scale T as the duration of the experiment. In the remainder of the paper, we will drop the asterisks for notational simplicity, and we will use the superscript $^{\dim}$ to denote the dimensional parameter corresponding to a given dimensionless parameter. With these rescalings, the dimensionless equations describing cell movement in the Boyden chamber are as follows:

$$\text{On } 0 < x < 1: \quad \frac{\partial n}{\partial t} = -\frac{\partial J_n}{\partial x} \tag{8a}$$

$$\frac{\partial c}{\partial t} = D_c \frac{\partial^2 c}{\partial x^2} + k_d \Gamma n \rho - k_a \Gamma c n[1 + (\beta - 1)\rho] \tag{8b}$$

$$\frac{\partial \rho}{\partial t} = -\frac{J_n}{n}\frac{\partial \rho}{\partial x} + k_a c[1 + (\beta - 1)\rho] - (k_d + k_i)\rho \tag{8c}$$

where

$$J_n = -(D_0 + D_1\rho - D_2\rho^2)\frac{\partial n}{\partial x} + \chi n \frac{\partial \rho}{\partial x}$$

$$\text{On } -h_L < x < 0$$

$$\text{and} \qquad 1 < x < h_U: \quad \frac{\partial c}{\partial t} = D_c \frac{\partial^2 c}{\partial x^2}. \tag{8d}$$

This parabolic–hyperbolic system of partial differential equations is subject to the following end conditions:

$$\text{At } t = 0: \quad n = 0 \quad \text{on } 0 \le x < 1, \; n = 1 \quad \text{at } x = 1$$
$$\rho = 0 \quad \text{on } 0 \le x \le 1$$
$$c = 1 \quad \text{on } -h_L \le x < 1, \qquad c = c_U \quad \text{on } 1 \le x \le h_U.$$

$$\text{At } x=0: \quad \frac{\partial n}{\partial t}=-J_n/L, \qquad \frac{\partial \rho}{\partial x}=0, \qquad \frac{\partial c}{\partial x} \text{ continuous}$$

$$\text{At } x=1: \quad \frac{\partial n}{\partial t}=J_n/L, \qquad \frac{\partial \rho}{\partial x}=0, \qquad \frac{\partial c}{\partial x} \text{ continuous}$$

$$\text{At } x=-h_L, h_U: \quad \frac{\partial c}{\partial x}=0$$

A typical solution of this system, for the values of the transport coefficients discussed below, is illustrated in Fig. 5. In this figure, it is not immediately clear that the end conditions on c and ρ at $x=0, 1$ are satisfied, but detailed numerical investigation confirms that these conditions do hold. In both cases, a wave of cell density moves through the filter during the experiment. The concentration of extracellular FMLP decreases with time owing to rapid binding and internalization of bound receptors at the cell surface, and after an initial rapid rise from zero, the number of these bound receptors per cell also decreases because at high levels of receptor occupancy, dissociation and internalization of the receptor–chemical complex occur slightly more rapidly

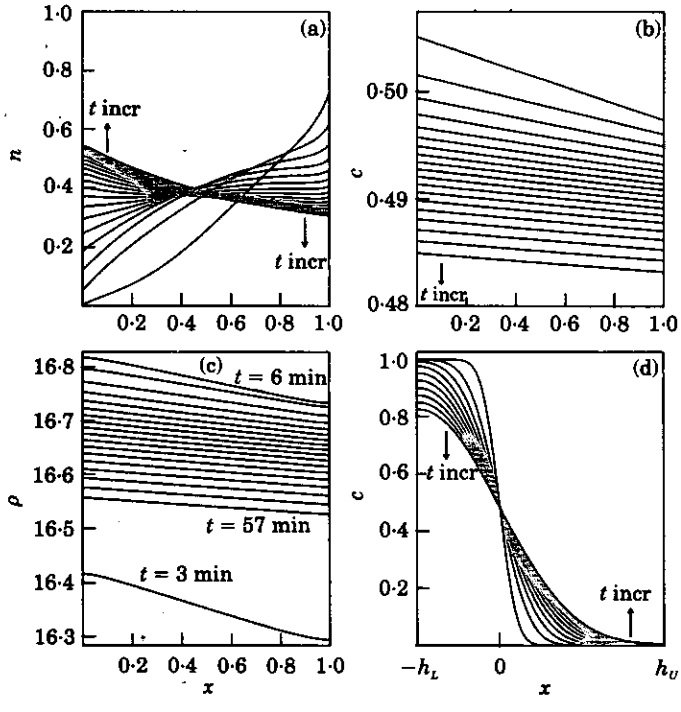

FIG. 5. The solution for $n(x, t)$, $c(x, t)$ and $\rho(x, t)$ of (8), plotted against x at equally spaced times. For clarity, we plot with time intervals of 3 min for the solutions within the filter, and 6 min for $c(x, t)$ in the wells. The parameter values are as discussed in the text, with $c_L=4\times10^{-8}$ M and $c_U=0$. The equations were solved numerically using the semi-implicit finite difference scheme discussed in the Appendix. (a) $n(x, t)$ in filter; (b) $c(x, t)$ in filter; (c) $\rho(x, t)$ in filter; (d) $c(x, t)$ in filter and wells.

than its association. In both cases, the spatial gradients of both extracellular chemical concentration and bound receptors per cell are quite small.

Comparison with Experimental Data

We have developed a model for chemically controlled cell movement based on chemical–receptor interactions on the cell surface, and we have used experimental data to obtain quantitative estimates for all the parameter values except the transport coefficients χ, D_0, D_1 and D_2. We now use data from the Boyden chamber experiments of Harvath & Aksamit (1984), illustrated in Fig. 2, to estimate these remaining parameters and to test the model.

In the absence of extracellular chemical, the model (8) reduces to a linear diffusion equation with diffusion coefficient D_0. Further, as the concentration of extracellular chemical becomes very large, the receptors on the cell surface become saturated with ligand, and thus ρ approaches its upper limit of $\rho_{\max}$ at all points in the filter. Thus in the limit as $c_L \to \infty$, the model again reduces to a linear diffusion equation, in this case with diffusion coefficient $(D_0 + D_1\rho_{\max} - D_2\rho_{\max}^2)$. Therefore the results of Harvath & Aksamit (1984) for $c_L = 0$ and c_L very large, together with their results for one intermediate concentration in both the cases $c_L = c_U^{\dim}$ and $c_L = 0$, enable all four transport coefficients to be estimated.

This approach gives the dimensional values $D_0^{\dim} = 1{\cdot}3 \times 10^{-10}\ \mathrm{cm^2\ sec^{-1}}$, $D_1^{\dim} = 4{\cdot}8 \times 10^{9}\ \mathrm{cm^2\ sec^{-1}\ mol^{-1}}$, $D_2^{\dim} = 3{\cdot}0 \times 10^{28}\ \mathrm{cm^2\ sec^{-1}\ mol^{-2}}$, and $\chi^{\dim} = 2{\cdot}0 \times 10^{12}\ \mathrm{cm^2\ sec^{-1}\ mol^{-1}}$. With these values, the model prediction of the dose–response curve for neutrophils and FMLP in the Boyden chamber used by Harvath & Aksamit (1984) is as illustrated in Fig. 6. These results capture the main qualitative

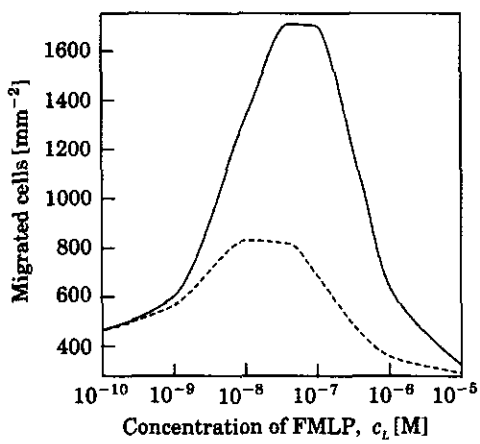

FIG. 6. The dose–response curve for human neutrophils and FMLP, as predicted by the model (8). The corresponding experimental result is illustrated in Fig. 2. The parameter values are as discussed in the text, and the equations were solved numerically using the semi-implicit finite difference scheme discussed in the Appendix. The final number of cells on the lower surface of the filter is determined as $n(0, 1) \cdot N_0$, where N_0 is the initial number of cells in the upper well. (—— $c_U^{\dim} = 0$; - - - $c_U^{\dim} = c_L$).

features of the corresponding experimental results (see Fig. 2). However, they do differ in quantitative detail. We anticipated such quantitative differences, since our model represents the increase in total receptor number with occupied receptor number, and the increase in cell flux with occupied receptor gradient, as linear. In reality, these processes are undoubtedly non-linear, but experimental data from which detailed relationships could be obtained are not currently available. Although we have not undertaken a detailed study, we expect that the fit between the model predictions and experimental data could be considerably improved by the introduction of appropriate non-linearities, in a manner similar to that used for the simple model that we considered initially. The key difference between the two models is that in the simple model, the introduction of appropriate non-linearities is crucial for the model predictions to be even qualitatively correct, whereas in our new model, any non-linearities are simply perturbing the model predictions about a basic form that is already qualitatively correct.

The model can also be tested against experimental results from a "leading front" Boyden chamber assay. In this approach, first used by Zigmond & Hirsch (1973), a thicker filter is used, and the distance travelled by the leading cell front is measured. The model can be applied to this assay exactly in the form (8); in Fig. 7, we compare the model predictions to the experimental results of Harvath & Aksamit (1989),

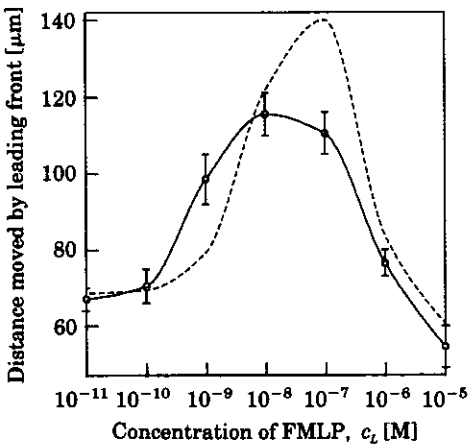

FIG. 7. The experimental results of Harvath & Aksamit (1989) from a "leading front" Boyden chamber assay, and the corresponding predictions of the model (8). The dimensions of the chamber were, in the notation of Fig. 1, $h_L = 3{\cdot}125$ mm, $h_U = 3{\cdot}75$ mm, $a = 150$ μm and $A = 8$ mm^2. In the experimental study, cellulose nitrate filters with 5 μm pores were used, 30 000 cells were added to the upper well, suspended in Hank's balanced salt solution with 0·2% bovine serum albumin; the peptide was also in solution with Hank's balanced salt solution. The chambers were incubated for 45 min at 37°C in humidified air. Harvath & Aksamit (1989) define the "cell front" as the position of the furthest horizontal cross-section of the filter containing at least three cells, and we therefore take the location of the front to be the position at which the cell density corresponds to three cells. The model parameter values are as discussed in the text, and the equations were solved numerically using the semi-implicit finite difference scheme discussed in the Appendix. The data points denote the mean experimental result, and the error bars represent the standard deviation of the means. (—— Experimental results; – – – model predictions.)

which again used the neutrophil–FMLP system. The cell transport coefficients are different in this study and that of Harvath & Aksamit (1984), primarily owing to differences in the material of the filter. The result for the control case $c_L = 0$ enables us to estimate D_0, giving the value $D_0^{\text{dim}} = 6{\cdot}1 \times 10^{-10}$ cm^2 sec^{-1}, and we assume that all the other transport coefficients are increased in the same proportion. In reality, different transport coefficients will increase to different extents, and more detailed data (in particular, data for the case $c_L = c_U^{\text{dim}}$) would enable us to estimate the other coefficients independently, which would improve the fit between the model predictions and experimental data. There are again quantitative differences between the results of the model and experimental data, but the model results again have the appropriate qualitative forms. Moreover, the form of the cell front was determined experimentally by Zigmond & Hirsch (1973), and although their experiments were for a different cell–chemical system, the shape of the front was very similar to that predicted by our model (results not shown).

Since our model depends on the kinetics of receptor–chemical binding, we can use experimental data on the variation of the kinetic parameters with temperature to predict dose–response curves at different temperatures. Although quantitative results are rare, a number of authors have found a decrease in neutrophil chemotaxis as temperature is decreased (for example, Nielsen & Olesen, 1983; Ternowitz, 1985). A number of the model parameter values are temperature dependent, in particular the three kinetic parameters k_a, k_i and k_d; the data of Sklar *et al.* (1984) enables the values of these parameters to be estimated at 15°C and 25°C, as well as 37°C. Experimental data suggest that the unstimulated random motility of neutrophils at 25°C is about half the value observed at 37°C (Olson, 1990). We therefore take D_0 at 25°C to be half the value at 37°C, and we assume that the other cell transport coefficients will be reduced by the same fraction. The chemical diffusion coefficient D_c will also be smaller at lower temperatures, which will in fact tend to increase the chemotactic response by increasing the local chemical concentration gradient; its value can be calculated at these lower temperatures using eqn (3). Under these assumptions, we calculated dose–response curves at 25°C for both the "leading front" and "migrated cell" assays, and our results are shown in Fig. 8. The predicted dose–response curves are markedly different from those at 37°C (see Figs 6 and 7), and the changes in the kinetic parameters are crucial to the new forms. To illustrate this point, we solved the model equations with D_c and the cell transport coefficients reduced to their values at 25°C, but with k_a, k_i and k_d at their 37°C values. We found that both the extent of the maximum chemotactic response and the concentration of FMLP giving this maximum response were significantly increased, for both assays, compared to the response illustrated in Fig. 8. Our model could be used in the same way to predict the effect on dose–response curves of other changes in experimental conditions, such as the pH in the Boyden chamber or the presence of a second, competing ligand.

Conclusion

The vast majority of continuum models for chemically controlled eukaryotic cell movement that are in current use are based on the seminal work of Keller & Segel

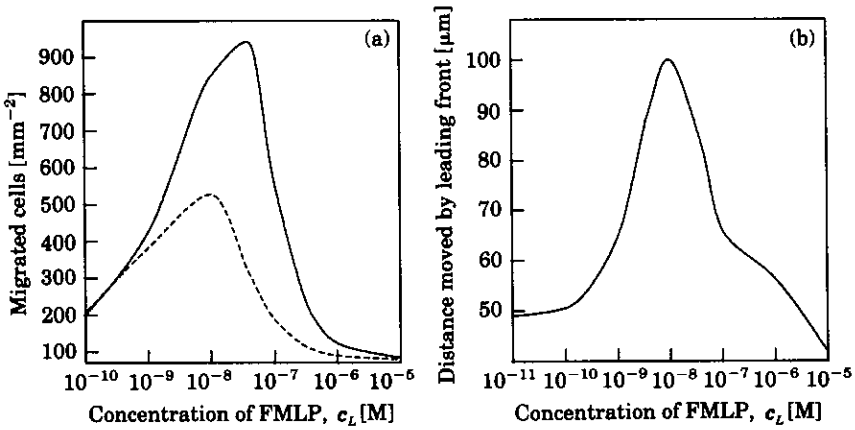

FIG. 8. The dose–response curves for human neutrophils and FMLP at 25°C, as predicted by the model (8), for (a) "migrated cell" and (b) "leading front" Boyden chamber assays. The dimensions of the chamber, the duration of the assay, and the total number of cells used are as in the experiments of Harvath & Aksamit (1984) and (1989), respectively, and as used in Figs 6 and 7, respectively. The dimensional model parameter values are $k_a^{\dim} = 8{\cdot}9 \times 10^8\ \mathrm{M}^{-1}\ \mathrm{min}^{-1}$, $k_d^{\dim} = 0{\cdot}02\ \mathrm{min}^{-1}$, $k_i^{\dim} = 0{\cdot}1\ \mathrm{min}^{-1}$, $D_c^{\dim} = 5{\cdot}5 \times 10^{-6}\ \mathrm{cm}^2\ \mathrm{sec}^{-1}$, $D_0^{\dim} = 6{\cdot}5 \times 10^{-11}\ \mathrm{cm}^2\ \mathrm{sec}^{-1}$, $D_1^{\dim} = 2{\cdot}4 \times 10^9\ \mathrm{cm}^2\ \mathrm{sec}^{-1}\ \mathrm{mol}^{-1}$, $D_2^{\dim} = 1{\cdot}5 \times 10^{28}\ \mathrm{cm}^2\ \mathrm{sec}^{-1}\ \mathrm{mol}^{-2}$, and $\chi^{\dim} = 10^{12}\ \mathrm{cm}^2\ \mathrm{sec}^{-1}\ \mathrm{mol}^{-1}$, with all other parameters as discussed in the text and as used in Figs 6 and 7. The model equations were solved numerically using the semi-implicit finite difference scheme discussed in the Appendix. (—— $c_U^{\dim} = 0$; – – – $c_U^{\dim} = c$.)

(1971*a*, *b*). These models have been highly successful in a wide range of applications. However, one drawback of the Keller–Segel approach is that it requires external specification of the variation of transport coefficients with chemical concentration. In this paper, we have proposed a new model which avoids this problem by incorporating the receptor kinetics on which these parameter variations depend. The model predictions capture the key qualitative features of the experimental dose–response curves for neutrophils and FMLP obtained from the Boyden chamber assay, through use of either the distance travelled by the cell front, or the total number of migrated cells, as a measure of stimulated cell motion. We have also used our model to predict dose–response curves for both types of assay at 25°C, and our results show that changes in the kinetic parameters play a key role in controlling the temperature dependence of cell chemotaxis and chemokinesis.

We would like to thank Dr Katherine Sprugel (Zymogenetics, Seattle, WA, U.S.A.) for initiating our interest in the Boyden chamber assay, Dr Endre Suli (Oxford University Computing Laboratory, U.K.) for his help with numerical solution of the model equations, and Dr Philip Maini (Centre for Mathematical Biology, Oxford, U.K.) for a number of helpful discussions. J.A.S. was supported in part by a graduate studentship from the Science and Engineering Research Council of Great Britain, and in part by a Junior Research Fellowship at Merton College, Oxford. This work was in part supported by Grant DMS-900339 from the U.S. National Science Foundation (J.D.M.) and in part by Grant GM-07441 from the National Institutes of Health (E.H.S.).

REFERENCES

BARROW, G. M. (1981). *Physical Chemistry for the Life Sciences.* New York: McGraw-Hill.

BERG, O. G. & VON HIPPEL, P. H. (1985). Diffusion-controlled macromolecular interactions. *Ann. Rev. Biophys. Biophys. Chem.* **14,** 131–160.

BIGNOLD, L. P. (1988*a*). Chemotaxis and chemokinesis of neutrophils: a reply. *J. Immunol. Meth.* **110,** 145–148.

BIGNOLD, L. P. (1988*b*). Measurement of chemotaxis of polymorphonuclear leukocytes *in vitro*. *J. Immunol. Meth.* **108,** 1–18.

BOYDEN, S. V. (1962). The chemotactic effect of mixtures of antibody and antigen on polymorphonuclear leukocytes. *J. exp. Med.* **115,** 453–466.

BUETTNER, H. M., LAUFFENBURGER, D. A. & ZIGMOND, S. H. (1989*a*). Measurement of leukocyte motility and chemotaxis parameters with the Millipore filter assay. *J. Immunol. Meth.* **123,** 25–37.

BUETTNER, H. M., LAUFFENBURGER, D. A. & ZIGMOND, S. H. (1989*b*). Cell transport in the Millipore filter assay. *Am. Inst. Chem. Eng. J.* **35,** 459–465.

CHARNICK, S. B., FISHER, E. S. & LAUFFENBURGER, D. A. (1991). Computer simulations of cell-target encounter including biased cell motion toward targets: single and multiple cell-target simulations in two dimensions. *Bull. math. Biol.* **53,** 591–621.

CHARNICK, S. B. & LAUFFENBURGER, D. A. (1990). Mathematical analysis of cell-target encounter rates in three dimensions. *Biophys. J.* **57,** 1009–1023.

DEVREOTES, P. N. & ZIGMOND, S. H. (1988). Chemotaxis in eukaryotic cells: a focus on leukocytes and *Dictyostelium*. *Ann. Rev. Cell Biol.* **4,** 649–686.

FISHER, E. S. & LAUFFENBURGER, D. A. (1987). Mathematical analysis of cell-target encounter rates in two dimensions. The effect of chemotaxis. *Biophys. J.* **51,** 705–716.

FLETCHER, M. P. & GALLIN, J. I. (1980). Degranulating stimuli increase the availability of receptors on human neutrophils for the chemoattractant f-Meu-Leu-Phe. *J. Immunol.* **124,** 1585–1588.

FOLLIN, P., DAHLGREN, C., BRIHEIM, G. & SANDSTEDT, S. (1989). Human neutrophil chemi-luminescence and f-meth-leu-phe receptor exposure in bacterial infections. *APMIS* **97,** 585–590.

GEX-FABRY, M. & DELISI, C. (1984). Receptor-mediated endocytosis: a model and its implications for experimental analysis. *Am. J. Physiol.* **247,** R768–R779.

GOLDBETER, A. & KOSHLAND, D. E. (1982). Simple molecular model for sensing and adaptation based on receptor modification with application to bacterial chemotaxis. *J. molec. Biol.* **161,** 395–416.

HARVATH, L. & AKSAMIT, R. R. (1984). Oxidised N-formylmethionyl-leucyl-phenylalanine: effect on the activation of human monocyte and neutrophil chemotaxis and superoxide production. *J. Immunol.* **133,** 1471–1476.

HARVATH, L. & AKSAMIT, R. R. (1989). Human granulocytes and granulocytes from other species demonstrate differences in chemotactic responsiveness to oxidized N-formyl-methionyl-leucyl-phenyl-alanine. *Comp. Biochem. Physiol.* **A92,** 97–100.

JANSSENS, P. M. W. & VAN DRIEL, R. (1984). *Dictyostelium discoideum* cell membranes contain masked chemotactic receptors for cyclic AMP. *FEBS Lett.* **176,** 245–249.

KELLER, E. F. & SEGEL, L. A. (1971*a*). Model for chemotaxis. *J. theor. Biol.* **30,** 225–234.

KELLER, E. F. & SEGEL, L. A. (1971*b*). Travelling bands of chemotactic bacteria: a theoretical analysis. *J. theor. Biol.* **30,** 235–248.

KEL'ER, H. U., WILKINSON, P. C., ABERCROMBIE, M., BECKER, E. L., HIRSCH, J. G., MILLER, M. E., RAMSEY, W. S. & ZIGMOND, S. H. (1977). A proposal for the definition of terms related to locomotion of leucocytes and other cells. *Clin. Exp. Immunol.* **27,** 377–380.

LAUFFENBURGER, D. A., TRANQUILLO, R. T. & ZIGMOND, S. H. (1988). Concentration gradients of chemotactic factors in chemotaxis assays. *Meth. Enzymol.* **162,** 85–101.

LAUFFENBURGER, D. A. & ZIGMOND, S. H. (1981). Chemotactic factor concentration gradients in chemotaxis assay systems. *J. Immunol. Meth.* **40,** 45–60.

LENTZ, T. L. (1971). *Cell Fine Structure.* Philadelphia: W. B. Saunders.

LINDERMAN, J. J. & LAUFFENBURGER, D. A. (1989). Receptor/ligand sorting along the endocytic pathway. *Lect. Notes Biomath* **78,** Berlin: Springer-Verlag.

MARTIEL, J. L. & GOLDBETER, A. (1987). A model based on receptor desensitization for cyclic-AMP signaling in *Dictyostelium* cells. *Biophys. J.* **52,** 807–828.

MONK, P. B. & OTHMER, H. G. (1989). Cyclic AMP oscillations in suspensions of *Dictyostelium discoideum*. *Phil. Trans. R. Soc. B.* **323,** 185–224.

NIELSEN, H. & OLESEN, L. S. (1983). Human monocyte chemotaxis *in vitro*. Influence of *in vitro* variables in the filter assay. *Acta. Pathol. Microbiol. Immunol. Scand. C* **91,** 109–115.

OLSON, D. P. (1990). *In vitro* migration responses of neutrophils from cows and calves. *Am. J. Vet. Res.* **51**, 973–977.

OMANN, G. M., ALLEN, R. A., BOKOSH, G. M., PAINTER, R. G., TRAYNOR, A. E. & SKLAR, L. A. (1987). Signal transduction and cytoskeletal activation in the neutrophil. *Physiol. Rev.* **67**, 285–322.

RIVERO, M. A., TRANQUILLO, R. T., BUETTNER, H. M. & LAUFFENBURGER, D. A. (1989). Transport models for chemotactic cell populations based on individual cell behaviour. *Chem. Eng. Sci.* **44**, 2881–2897.

SEGEL, L. A. (1976). Incorporation of receptor kinetics into a model for bacterial chemotaxis. *J. theor. Biol.* **57**, 23–42.

SEGEL, L. A. (1977). A theoretical study of receptor mechanisms in bacterial chemotaxis. *SIAM J. Appl. Math.* **32**, 653–665.

SEGEL, L. A., GOLDBETER, A., DEVREOTES, P. N. & KNOX, B. E. (1986). A mechanism for exact sensory adaptation based on receptor modification. *J. theor. Biol.* **120**, 151–179.

SKLAR, L. A., FINNEY, D. A., OADES, Z. G., JESAITIS, A. J., PAINTER, R. G. & COCHRANE, C. G. (1984). The dynamics of ligand receptor interactions. *J. Biol. Chem.* **259**, 5661–5669.

SMITH, G. D. (1985). *Numerical Solution of Partial Differential Equations: Finite Difference Methods.* Oxford: Clarendon Press.

SULLIVAN, S. J. & ZIGMOND, S. H. (1980). Chemotactic peptide receptor modulation in polymorphonuclear leukocytes. *J. Cell Biol.* **85**, 703–711.

TATSUO, E. & KOBAYASHI, S. (1972). *Fine Structure of Human Cells and Tissues.* Tokyo: Igaku Shoin.

TERNOWITZ, T. (1985). Human monocyte and neutrophil chemotaxis *in vitro* employing 51Cr-labelled leukocytes. *Acta. Pathol. Microbiol. Immunol. Scand. C* **93**, 189–193.

TRANQUILLO, R. T. (1990). Theories and models of gradient perception. In: *Biology of the Chemotactic Response* (Armitage, J. P. & Lackie, J. M., eds) pp. 35–75. Cambridge: Cambridge University Press.

TRANQUILLO, R. T. & LAUFFENBURGER, D. A. (1987). Stochastic model of leukocyte chemosensory movement. *J. math. Biol.* **25**, 229–262.

TRANQUILLO, R. T. & LAUFFENBURGER, D. A. & ZIGMOND, S. H. (1988). A stochastic model for leukocyte random motility and chemotaxis based on receptor binding fluctuations. *J. Cell Biol.* **106**, 303–309.

TYSON, J. J. & MURRAY, J. D. (1989). Cyclic AMP waves during aggregation of *Dictyostelium* amoebae. *Development* **106**, 421–426.

VAN HAARSTERT, P. J. M. (1987). Down-regulation of cell surface cyclic AMP receptors and desensitization of cyclic AMP-stimulated adenylate cyclase by cyclic AMP in *Dictyostelium discoideum*. Kinetics and concentration dependence. *J. Biol. Chem.* **262**, 7700–7704.

WILKINSON, P. C. (1988*a*). Chemotaxis and chemokinesis: confusion about definitions. *J. Immunol. Meth.* **110**, 143–144.

WILKINSON, P. C. (1988*b*). Reply to the letter of L. P. Bignold. *J. Immunol. Meth.* **110**, 149.

WILLIAMS, L. T., SNYDERMAN, R., PIKE, M. C. & LEFKOWITZ, R. J. (1977). Specific receptor sites for chemotactic peptides on human polymorphonuclear leukocytes. *Proc. natn. Acad. Sci. U.S.A.* **74**, 1204–1208.

ZIGMOND, S. H. (1981). Consequences of chemotactic peptide receptor modulation for leukocyte orientation. *J. Cell. Biol.* **88**, 644–647.

ZIGMOND, S. H. (1989). Cell locomotion and chemotaxis. *Curr. Opin. Cell Biol.* **1**, 80–89.

ZIGMOND, S. H. & HIRSCH, J. G. (1973). Leukocyte locomotion and chemotaxis: new methods for evaluation and demonstration of a cell-derived chemotactic factor. *J. exp. Med.* **137**, 387–410.

ZIGMOND, S. H., SULLIVAN, S. J. & LAUFFENBURGER, D. A. (1982). Kinetic analysis of chemotactic peptide receptor modulation. *J. Cell Biol.* **92**, 34–43.

ZIMMERLI, W., SELIGMANN, B. & GALLIN, J. I. (1986). Exudation primes human and guinea pig neutrophils for subsequent responsiveness to chemotactic peptide N-formylmethionylleucyl-phenylalanine and increases complement component C3bi receptor expression. *J. Clin. Invest.* **77**, 925–933.

APPENDIX

In this Appendix, we discuss the numerical solution of the dimensionless model eqn (8). The equations are a parabolic–hyperbolic system, and are thus rather non-standard, so that particular care is required when solving numerically. We have investigated a number of possible discretizations of the system (8), both explicit and

implicit in time, and we have found a semi-implicit scheme to be the most efficient. Using subscripts to denote the space node and superscripts to denote the time point, the scheme in the filter region $0<x<1$ is as follows:

$$\frac{n_i^{j+1}-n_i^j}{\delta t}=(D_0+D_1\rho_i^j-D_2\rho_i^{j2})\left(\frac{n_{i+1}^{j+1}-2n_i^{j+1}n_{i-1}^{j+1}}{\delta x^2}\right)-\chi n_i^j\left(\frac{\rho_{i+1}^j-2\rho_i^j+\rho_{i-1}^j}{\delta x^2}\right)$$

$$+(D_1-2D_2\rho_i^j-\chi)\left(\frac{n_{i+1}^j-n_{i-1}^j}{2\delta x}\right)\left(\frac{\rho_{i+1}^j-\rho_i^j}{\delta x}\right)$$

$$\frac{c_i^{j+1}-c_i^j}{\delta t}=D_c\left(\frac{c_{i+1}^{j+1}-2c_i^{j+1}+c_{i-1}^{j+1}}{\delta x^2}\right)+k_d\Gamma n_i^j\rho_i^j-k_a\Gamma c_i^j n_i^j[1+(\beta-1)\rho_i^j]$$

$$\frac{\rho_i^{j+1}-\rho_i^j}{\delta t}=\left[(D_0+D_1\rho_i^j-D_2\rho_i^{j2})\left(\frac{n_{i+1}^j-n_{i-1}^j}{2n_i^j\delta x}\right)-\chi\left(\frac{\rho_{i+1}^j-\rho_i^j}{\delta x}\right)\right]\left(\frac{\rho_{i+1}^j-\rho_i^j}{\delta x}\right)$$

$$+k_a c_i^j[1+(\beta-1)\rho_i^j]-(k_d+k_i)\rho_i^j.$$

Here δx is the node separation in the uniform space mesh, and δt is the time step. The use of a forward difference representation of $\partial\rho/\partial x$ is crucial: central and backwards difference approximations both give unstable schemes. This is familiar from the theory of numerical solution of first-order partial differential equations (Smith, 1985: chapter 4), and is to be expected since (8c) is first order in ρ. The diffusion equation (8d) for the chemical concentration $c(x, t)$ in the wells was solved using a fully implicit time discretization. The overall scheme then gives a tridiagonal system of linear equations, which can be solved very efficiently by Gaussian elimination.